

Dynamic response and hysteresis dispersion scaling of ferroelectric SrBi₂Ta₂O₉ thin films

B. Pan, H. Yu, D. Wu, X. H. Zhou, and J.-M. Liu^{a)}

Laboratory of Solid State Microstructures, Nanjing University, Nanjing 210093, China and International Center for Materials Physics, Chinese Academy of Sciences, Shenyang, China

(Received 22 April 2003; accepted 19 June 2003)

The dynamic hysteresis response of ferroelectric SrBi₂Ta₂O₉ thin films versus periodically varying electric field over a frequency range of $f=10^{-1}$ – 10^6 Hz and amplitude range of $E_0 = 15$ – 158 kV/cm is measured utilizing the Sawyer–Tower method. The dynamic order parameter Q shows anomalous behavior against the field amplitude, and a single-peaked hysteresis dispersion is identified. The field response of hysteresis area $\langle A \rangle$ in the form of $\langle A \rangle \propto f^{2/3} E_0^{2/3}$ over the low frequency range is evaluated, while the response over the high frequency range takes the form of $\langle A \rangle \propto f^{-1/3} E_0^2$. We demonstrate that the hysteresis dispersion spectrum exhibits single-parameter scaling, and predicts a characteristic time for domain reversal that is inversely correlated to the field amplitude. © 2003 American Institute of Physics. [DOI: 10.1063/1.1602580]

A significant amount of research and development has focused on ferroelectric thin films for high-speed ferroelectric (FE) random access memories (RAMs) and other advanced FE-based electronic devices.^{1,2} One of the essential problems in these studies are the dynamics of ferroelectric domain reversal, i.e., the response of domain reversal versus time-varying external electric field E .³ It is well understood that domain reversal depends significantly on amplitude E_0 and frequency f of field E . The dynamic hysteresis, i.e., hysteresis area $\langle A \rangle$ as a function of E_0 and f , presents quite a lot of information on the dynamics, because $\langle A \rangle$ scales the energy dissipation within one period of domain reversal.³ Among the numbers of ferroelectrics, bismuth layer-structured ferroelectric materials have attracted great interest and SrBi₂Ta₂O₉ (SBT) has been demonstrated on the industrial scale for FE-RAM applications, because of its nonfatigue nature against domain reversal with a simple metal electrode such as Pt and low polarization switching voltage.³ The purpose of this letter was to study the dynamic hysteresis of ferroelectric SBT thin films.

One of the well-known theoretical predictions of dynamic hysteresis is given by the three-dimensional $(\phi^2)^2$ or $(\phi^2)^3$ model with $O(N)$ symmetry in a large N limit,^{4,5} which reads over extremely low and high ranges of frequency

$$\begin{aligned} \langle A \rangle &\propto f^{1/3} E_0^{2/3} \text{ as } f \rightarrow 0, \\ \langle A \rangle &\propto f^{-1} E_0^2 \text{ as } f \rightarrow \infty. \end{aligned} \quad (1)$$

We first check whether Eq. (1) can be applied to SBT thin films or not. On the other hand, similar to ferromagnetics, the domain reversal in ferroelectrics can also be explained by the nucleation and growth concept.⁶ Under a dc field E , the nucleation rate of new domains and domain boundary motion velocity can be described by characteristic times t_n and t_g , respectively. The kinetics of domain reversal may be de-

finied by a third characteristic time, $t_c \sim (t_n \cdot t_g)^{1/2}$, i.e., the so-called effective time.⁷ For an ac field $E(t)$, say, $E(t) = E_0 \sin(2\pi ft)$ where t is time, if time t_e exists uniquely, the hysteresis dispersion $\langle A \rangle(f)$ at a given E_0 should be single peaked and scalable.⁸ The scaling behavior of the hysteresis dispersion for SBT thin films would be the second issue of the present study.

The SBT thin films used in this study were prepared by metalorganic decomposition (MOD) with a spin-coating technique. Carboxylate liquid precursors were spin coated onto oxidized Si substrates coated with a bottom electrode consisting of a thin TiO₂ adhesion layer and a sputter-deposited Pt film. The films were baked in air at 500 °C. A 60 min final stage annealing at 750 °C in flowing O₂ was conducted to crystallize the amorphous film. Pt top electrodes 200 μm in diameter were then sputter deposited on the SBT surface. The thin films show an average grain size of 100 nm and a thickness of 400 nm with preferred (115) orientation.

The dynamic hysteresis was measured using the Sawyer–Tower (ST) method, details of which were described earlier.⁹ For ST measurement, reliable calibration of the data is essential. We compare the ST data and the data obtained by a standard ferroelectric testing unit, the RT6000HVS (Radiant Technologies Inc., NM) at a cycle of 112 ms (corresponding to $f \sim 10$ Hz), shown in Fig. 1(a). The two loops are very consistent with respect to each other, demonstrating the applicability of the ST method.

In Figs. 1(b) and 1(c) are the as-measured hysteresis loops at different f but fixed E_0 , and at different E_0 but fixed f , respectively. As expected, the dependence of the loop pattern and area $\langle A \rangle$ on f and E_0 is remarkable. From Fig. 1(b) where E_0 is fixed, one sees the evolution of the pattern at different f . At lower f , such as at $f = 12$ Hz, the pattern is regular with low coercive field E_c and remanent polarization P_r . With a further increase of f , the loop becomes enlarged by increasing P_r and E_c . As f is quite high, 60 kHz, the loop begins to shrink, first by an increase of E_c but a decrease of P_r , and then by decreases of both E_c and P_r . The loop looks more saturated at $f = 1$ kHz than at $f = 12$ kHz. At f

^{a)}Author to whom correspondence should be addressed; electronic mail: liujm@nju.edu.cn

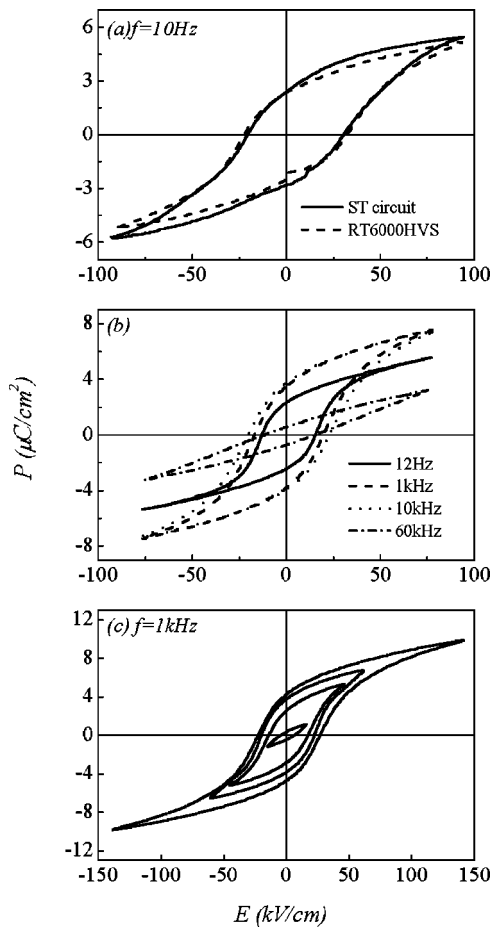


FIG. 1. Hysteresis loops measured (a) by the ST method and the RT6000HVS testing unit, (b) by the ST method at $E_0=75$ kV/cm and four different frequencies, and (c) by the ST method at $f=1$ kHz and four different amplitudes.

=60 kHz and higher, the hysteresis finally evolves into an unsaturated shape with very small P_r . Figure 1(c) shows that given a frequency of $f=1$ kHz, loop area $\langle A \rangle$, P_r , and E_c increase with an increase of E_0 over the f range covered until well saturated hysteresis.

The hysteresis evolution mentioned above can also be characterized by the amplitude dependence of dynamic order parameter Q defined as $Q = \omega/2\pi \oint P \cdot dt$,⁶ as shown in Fig. 2(a) by one example at $f=100$ Hz. The sample was initially in an unpoled state and E_0 was increased from 0 to 150 kV/cm. Then measurement was performed in reverse order. For ferromagnetic systems, Q falls monotonously down to zero from a nonzero value, corresponding to the case of a prepoled sample. However, for ferroelectrics, as least for SBT thin films on Pt coated silicon wafers, low E_0 applied to the unpoled sample leads to partial dynamic alignment of the domains. This alignment is further preferred with increasing E_0 but not all domains can be effectively reversed under such a low antiparallel field. This results in an enhanced Q value until the maximum at $E_0 \sim 100$ kV/cm which is much higher than E_c for SBT thin films. After this, the value of Q decays rapidly with increasing E_0 , indicating perfect domain reversal. More surprisingly, when E_0 decreases from 150 to 0 kV/cm, $Q(E_0)$ remains the same as that observed for E_0 increases. One possible mechanism responsible for this effect is that full alignment of domains cannot be reached unless a

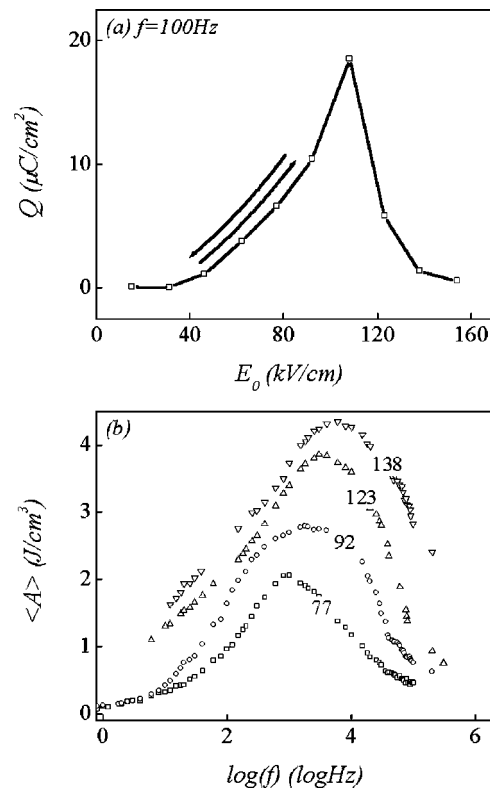


FIG. 2. (a) Dynamic order parameter Q as a function of amplitude E_0 at $f=100$ Hz and (b) hysteresis area $\langle A \rangle$ as a function of frequency f at four different amplitudes.

field of ~ 100 kV/cm is applied, and some of the domains may rebound back to their original orientations once the field is removed.

In Fig. 2(b) are several hysteresis dispersion curves $\langle A \rangle(f)$ at different E_0 . It is clearly seen that all dispersion curves exhibit the single-peaked pattern with features similar to those revealed earlier, on which detailed discussion can be found.^{7,8} To check the applicability of Eq. (1), one fits the low- f and high- f data with $\langle A \rangle \propto f^m E_0^n$ where m and n are exponents to be determined. It is revealed that rather than using Eq. (1), the low- f and high- f data can be much better fitted by $\langle A \rangle \propto f^{2/3} E_0^{2/3}$ and $\langle A \rangle \propto f^{-1/3} E_0^2$, respectively. This indicates that area $\langle A \rangle$ grows more quickly with f over the low- f range, and decays more slowly with f over the high- f range than the theoretical prediction, Eq. (1). It is interesting that exponent n as estimated is the same as the theoretical prediction, suggesting no significant effect of the very low E_c on dynamic hysteresis. The best fits of the results are presented in Fig. 3(a) and 3(b), respectively. We thus suggest that the dynamic hysteresis in SBT thin films does not follow the $(\Phi^2)^2$ or $(\Phi^2)^3$ model.

To check the single-parameter scalability of dispersion $\langle A \rangle(f)$ at different E_0 , we note that for all cases $\langle A \rangle(f)$ exhibits a single-peaked pattern with the peak position shifting gradually with an increase of E_0 . The shape of dispersions remains similar from one to another, just like the structure function of quenched binary alloys annealed over time.⁸ To proceed with the scaling analysis, we redefine the dispersion using $\log(f)$ as a variable and process the following scaling parameter:⁸

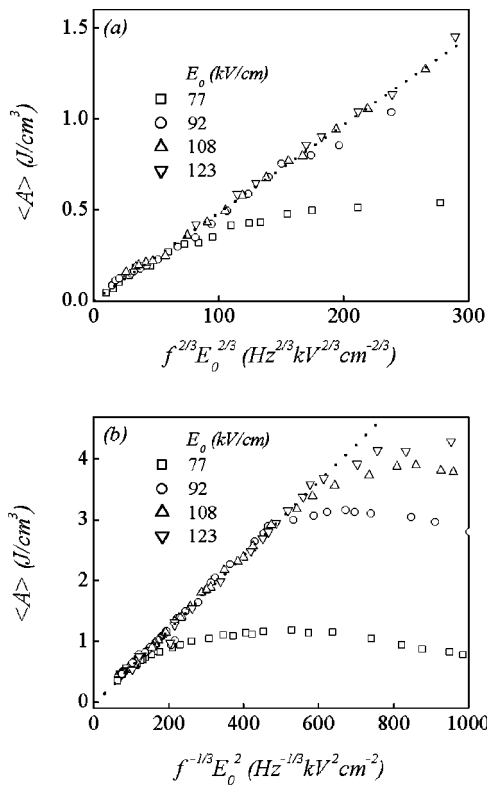


FIG. 3. Frequency response of hysteresis area $\langle A \rangle$ vs (a) $f^{2/3}E_0^{2/3}$ over the low-frequency range and (b) $f^{-1/3}E_0^2$ over the high-frequency range.

$$\gamma = \log(f),$$

$$S_n(E_0) = \int_{-\infty}^{\infty} \gamma^n \langle A \rangle(\gamma, E_0) d\gamma, \quad n = 1, 2, \dots,$$

$$\gamma_n(E_0) = S_n(E_0)/S_0(E_0), \quad (2)$$

$$n_2(E_0) = \gamma_2(E_0)/\gamma_1^2(E_0),$$

$$\tau_1^{-1} = 10^{\gamma_1},$$

where γ is the modified frequency, γ_n is the n th characteristic frequency, and τ_1 is the effective characteristic time by which to characterize the domain reversal dynamics. Estimated parameters τ_1 and n_2 as a function of E_0 are given in Fig. 4(a). Apart from the very small E_0 , scaling factor $n_2(E_0)$ remains almost unchanged. This independence predicts the scalability of dispersion $\langle A \rangle(\gamma)$ by the one-parameter scaling function, which reads

$$W(\eta) = \tau_1 \langle A \rangle(\gamma, E_0),$$

$$\eta = \log(f \cdot \tau_1). \quad (3)$$

Plotting all data on $W(\eta)$ estimated by the above scaling transform, shown in Fig. 4(b), shows that apart from cases of very small E_0 , all data fall onto the same curve within numerical uncertainty, demonstrating the dynamic scaling behavior of hysteresis dispersion. The scaling behavior also indicates that there indeed exists a unique characteristic time τ_1 for domain reversal, by which dynamic hysteresis can be uniquely characterized. The characteristic time τ_1 is propor-

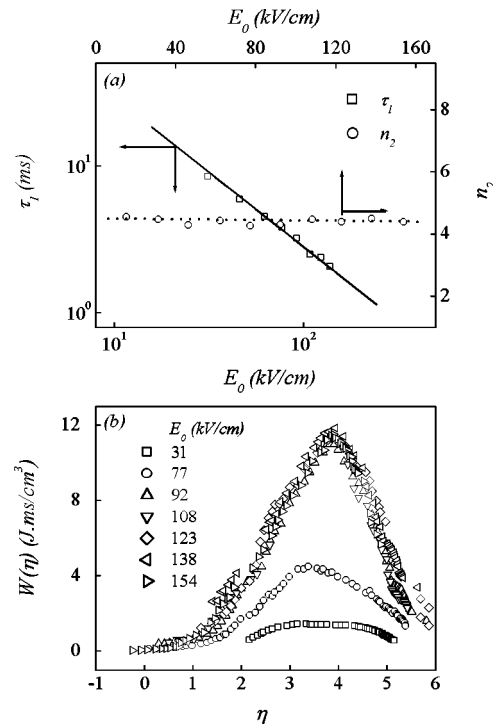


FIG. 4. (a) Characteristic time τ_1 and scaling factor n_2 as a function of amplitude E_0 and (b) scaling function $W(\eta)$ as a function of scaling variable η .

tional to the time t_e mentioned earlier. As a function of E_0 , it satisfies relation the $\tau_1 \propto E_0^{-1}$ in a satisfactory manner as long as E_0 is not very small, like in Fig. 4(a).⁸

In summary, we have studied in detail the dynamic hysteresis and scaling of the hysteresis dispersion in ferroelectric $\text{SrBi}_2\text{Ta}_2\text{O}_9$ thin films. The field response relations, $\langle A \rangle \propto f^{2/3}E_0^{2/3}$, over the low-frequency range and $\langle A \rangle \propto f^{-1/3}E_0^2$ over the high-frequency range have been estimated by Sawyer–Tower measurement. We have demonstrated the scaling property of hysteresis dispersion, and predicted the existence of an effective unique characteristic time which is inversely proportional to the amplitude of the field applied as long as the latter is not very small.

The authors would like to acknowledge the financial support of the National Key Project for Basic Research of China (2002CB613303), NSFC through the innovative group project and a normal project, as well as the Laboratory of Solid State Microstructures of Nanjing University.

¹J. F. Scott and C. A. Araujo, *Science* **246**, 1400 (1989).

²B. A. Tuttle, In *Thin Film Ferroelectric Materials and Devices*, edited by R. Ramesh (Kluwer Academic, Boston, 1997), p. 115.

³J. F. Scott, *Ferroelectric Memories* (Springer, Berlin, 2000).

⁴M. Rao, H. R. Krishnamurthy, and R. Pandit, *Phys. Rev. B* **42**, 856 (1990).

⁵M. Rao and R. Pandit, *Phys. Rev. B* **43**, 3373 (1991); Y.-H. Kim and J.-J. Kim, *ibid.* **55**, R11933 (1997).

⁶B. K. Chakrabarti and M. Acharyya, *Rev. Mod. Phys.* **71**, 847 (1999).

⁷J.-M. Liu, H. L. W. Chan, C. L. Choy, Y. Y. Zhu, S. N. Zhu, Z. G. Liu, and N. B. Ming, *Appl. Phys. Lett.* **79**, 236 (2001).

⁸J.-M. Liu, H. L. W. Chan, C. L. Choy, and C. K. Ong, *Phys. Rev. B* **65**, 014416 (2001).

⁹J.-M. Liu, H. P. Li, C. K. Ong, and L. C. Lim, *J. Appl. Phys.* **86**, 5198 (1999).